

Diagnostics From Three Rising Submillimeter Bursts

A. H. Zhou^{1,2}, J. P. Li^{1,2} and X. D. Wang³

¹ Key Laboratory of Dark Matter and Space Astronomy, Chinese Academy of Sciences;

zhouah@pmo.ac.cn

² Purple Mountain Observatory, Chinese Academy of Sciences, Nanjing 210008

³ Hohai University, Nanjing 210098, China

Abstract In the paper we investigate three novel rising submillimeter (THz) bursts occurred sequentially in a super-Active Region NOAA 10486. The average rising rate of the flux density above 200 GHz is only 20 sfu/GHz (corresponding spectral index α of 1.6) for the THz spectral components of 2003 October 28 and November 4 bursts, while it can attain values of 235 sfu/GHz ($\alpha=4.8$) for 2003 November 2 burst. The steeply rising THz spectrum can be produced by a population of high relativistic electrons with a low-energy cutoff of 1 MeV, while it only requires a low-energy cutoff of 30 keV for the two slowly rising THz bursts, via gyrosynchrotron (GS) radiation based on our numerical simulations of burst spectra in the magnetic dipole field case. The electron density variation is much larger in the THz source than that in microwave (MW) one. It is interesting that the THz source radius decreased by 20–50% during the decay phase for the three events, but the MW one increased by 28% for the 2003 November 2 event. In the paper we will present a calculation formula of energy released by ultrarelativistic electrons, accounting the relativistic correction for the first time. We find that the energy released by energetic electrons in the THz source exceeds that in microwave one due to the strong GS radiation loss at THz range, although the modeled THz source area is 3–4 orders smaller than the modeled MW one. The total energies released by energetic electrons via the GS radiation in radio sources are estimated, respectively, to be 5.2×10^{33} , 3.9×10^{33} and 3.7×10^{32} erg for the October 28, November 2 and 4 bursts, which are 131, 76 and 4 times as large as the thermal energies of 2.9×10^{31} , 2.1×10^{31} and 5.2×10^{31} erg estimated from the soft x-ray GOES observations.

Key words: Sun: submillimeter emission–Sun: energetic electrons–Sun: radio source environment

1 INTRODUCTION

Solar flares are a consequence of magnetic instabilities in the solar flare regions. During the flares, a large

tromagnetic radiation is emitted. So one of the most direct diagnostic of energetic (~ 1 MeV) electrons accelerated during solar flares is their GS radiation at centimeter-millimeter wavelengths emitted in magnetic loops associated with the flaring active region (e.g., Pick et al. 1990; Bastain et al. 1998). Before the year 2000 no radio observations above 90 GHz were available. At such frequencies the characteristic energy of radiating electrons is of a few MeV (e.g., Dulk 1985; Ramaty et al. 1994). Since 2000 new instrumentation observing in the 200–400 GHz range has become available, more than 10 flares have been observed in this band (l  thi et al. 2004a; l  thi et al. 2004b; Silva et al. 2007; Krucker et al. 2013).

It is interesting that among of them three strong submillimeter bursts occurred in succession in the same super-Active Region NOAA 10486 on 2003 October 28, November 2 and 4. For the three events, all the radio spectrum above 200 GHz are not the continuation of the GS spectrum measured at lower frequencies, but surprisingly increases with increasing frequency (l  thi et al. 2004a; Kaufmann et al. 2004; Silva et al. 2007; Trottet et al. 2008). This spectral feature is termed a "THz component". The positive-slope THz bursts have been observed thus far in only a handful of the most energetic events (Krucker 2013). So the three THz burst observations occurred in the same active region are very valuable.

The Terahertz wavelength range (0.1-10 THz) is a frontier observational window and its act is not replaced by other wavelength range, because it can provide unique diagnostics about energy release of ultrarelativistic electrons and their environment in lower atmosphere levels from 1000 to 30,000 km above the photosphere in flare regions. The THz events occurred on 2003 November 4 and 2 have been studied briefly (Zhou et al. 2010; Zhou et al. 2011). In the paper we will investigate the 2003 October 28 event in detail. We have carried out a sequence of numerical simulations for the spectral observations, using our GS emission model in the magnetic dipole field case (Zhou et al. 2008).

In the paper we will present, for the first time, a calculation formula of energy released by energetic electrons in the THz emission region, including the relativistic correction. We will use it to obtain the estimation of the energy released by energetic electrons in THz and MW emission regions for the three THz events. The total non-thermal energy released by energetic electrons in the radio wavelength range and thermal energy estimated from the soft x-ray GOES observations have been estimated and compared for the three bursts. Finally we present discussions and conclusions.

2 OBSERVATIONS

Extensive flare activities were observed in a super-AR NOAA 10486 during its disk passage of October 22 – November 4, 2003. Among them an extremely energetic 4B/X17.2 flare on October 28, 2003/11:10 was observed when the active region was located at S16 E08, i.e., close to the disk-center. The flare was rated the third large X-ray flare recorded by GOES satellite and the largest optical class (4B) flare observed so far. It is associated with a large MW and a rising THz burst. Emission at 210 GHz was first detected by the K  ln Observatory for Submillimeter and millimeter Astronomy (KOSMA) as a slow rise in intensity at $\sim 11:00$ UT (L  thi et al. 2004a; Trottet et al. 2008), i.e, ten minutes before at the onset of the flare. After a dramatic increase at $\sim 11:02:30$ UT, enormous peak flux densities of 25,000 and 11,000 sfu were reached

Table 1 Three Novel Rising THz Burst Observations in the AR 10486.

Date	H_α	$X - ray$	Position	$S_{MW}(sfu)$	$S_{\sim 200G}(sfu)$	$S_{405GHz}(sfu)$
10 28 2003/11:02	4B	$X_{17.2}$	S16E08	$S_{90GHz} : 25000$	11000	
11 02 2003/17:16	2B	$X_{8.3}$	S18W56	$S_{18GHz} : 35000$	4000	70000
11 04 2003/19:42	3B	$X_{\geq 28}$	S19W83	$S_{18GHz} : 48000$	11500	20000

The second rising THz burst in AR 10486 was detected by the Solar Submillimeter Telescope (SST) at 212 and 405 GHz (Silva et al. 2007) in the flare on November 2, 2003 starting at $\sim 17:16$ UT. This flare is classified as an X8.3 and 2B event. Their peak flux densities reached values of about 4,000 and 70,000 sfu at 212 and 405 GHz respectively. When the active region passed the west limb of the solar disk, the third large rising THz burst was observed by SST on November 4, 2003/19:42 UT (Kaufmann et al. 2004). It was associated with an $X_{\geq 28}$ flare (Kane et al. 2005), which may have been the largest X-ray event since observations began in 1976. The peak flux densities at 18 and 212 GHz attained, respectively, values of 48,000 and 11,500 sfu at the maximum phase (see Table 1).

3 RISING RATE OF FLUX DENSITY OF SUBMILLIMETER SPECTRUM

For the rising THz burst on October 28, emission at 210 GHz was detected as a slow rise in intensity at $\sim 11:00$ UT. The total flux density time profile exhibits a slowly varying, time-extended component from an extended source and a short-lived component from a compact source exhibiting three distinctive peaks. However there are no significant differences between the spectra emitted by the extended and the compact sources (Lüthi et al. 2004a). The flux density at 210 GHz increased from 3,100 to 11,000 sfu in a period of 11:03:15 to 11:05:25 UT at the rise phase, but the 230 and 345 GHz KOSMA-channels were saturated at these times due to the enormous flux density of the burst. So the corresponding flux densities have not been recorded at 230/345 GHz during the main phase. Figure 1 shows the temporal evolution spectra of this event given by Lüthi et al. (2004a).

The rise rate r of the flux density measured from the observation spectra is in the 18.5-8.5 sfu/GHz range during the October 28 burst (see Table 2), i.e., it is a slowly rising THz burst. The second THz burst occurred on November 4, exhibiting four peaks. Its rising rates of the flux density are also given in Table 2. It shows that for the 2003 November 4 event, r value variation is in the range of 7.8–44 sfu/GHz, which means that it is also a slowly rising THz burst. Their average rising rate reaches only 20 sfu/GHz (corresponding spectral index α of 1.6) for the two events. The rising rates of a steeply rising THz burst of the 2003 November 2 event were estimated (Li et al. 2015). Its average rise rate can attain a value of 235 sfu/GHz ($\alpha=4.8$) for 2003 November 2 burst, which is about one order of magnitude higher than that for the two slowly rising THz burst.

4 FITS OF THE THREE RISING SUBMILLIMETER BURST SPECTRA

It is well known that radio spectrum can provide crucial information about energetic electrons and their environment in solar flares. The information contains mainly the energy spectral index δ , low-energy and high-energy cutoffs E_0 and E_m , electron number density N , source size, and magnetic field strength B in

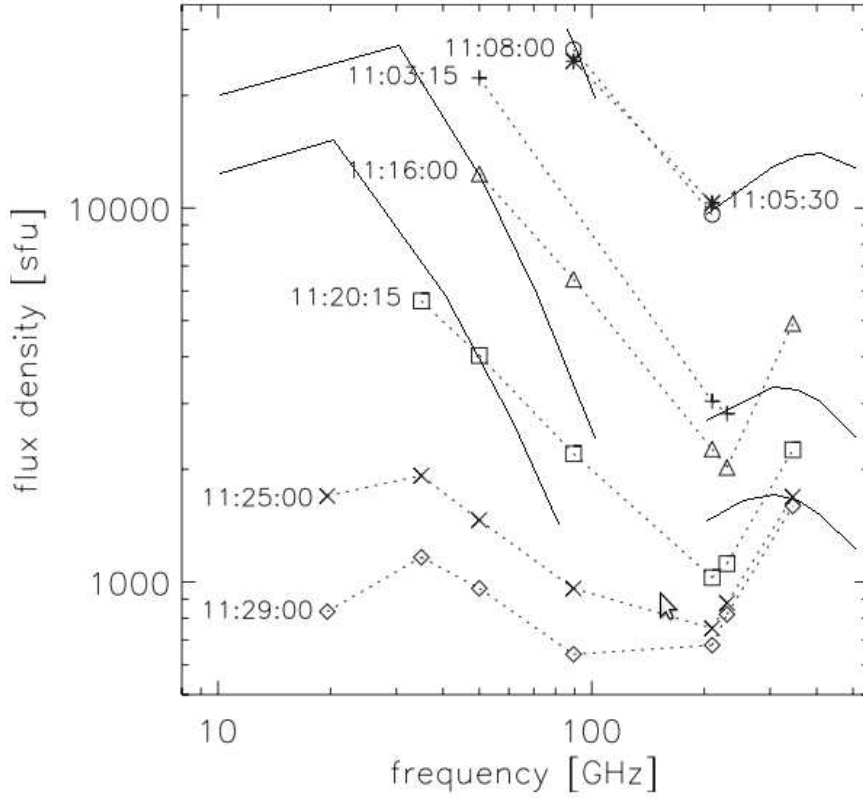


Fig. 1 The temporal evolutions of radio spectra of the October 28 burst given by Lüthi et al. (2004a) and for their fits (see the solid lines).

4.1 For the two slowly rising THz bursts

Here we will model the slowly rising THz spectral components of the 2003 October 28 burst for the first time. For this rising THz burst, the flux density at 210 GHz increased from 3,100 to 11,000 sfu at the rise phase but the corresponding higher frequency ($\nu > 210 \text{ GHz}$) observations have not been obtained during the main phase. So we only can estimate what condition, at least, can produce the rising THz spectral component with 11,000 sfu flux density at 210 GHz at the maximum phase via the GS emission, which leads to that the modeled spectrum is underestimated largely. It is well known that the low-energy cutoff and electron density can affect substantially the spectral calculations, so we selected, respectively, a sequence of low-energy cutoffs E_0 and a sequence of electron number densities N to model THz burst spectra for $E_m = 10 \text{ MeV}$. We find from these spectral calculations that the best set of values for the THz burst spectral fit at 11:05:30 UT of the maximum phase are for the low-energy cutoff of 30 keV and the number density of $4.5 \times 10^{10} \text{ cm}^{-3}$, where $\delta=2$, $B_0 = 5000 \text{ G}$, $\theta = 10^\circ$, and $h_d = 10^8 \text{ cm}$. The another two THz spectra at 11:16:00 and 11:20:15 UT at the decay phase also are fitted. The modeled THz and MW emission spectra are given in Figure 1 in the case of magnetic dipole field, which are superimposed on the original Figure 10 (dotted lines) given by Lüthi et al. (2004a). It is shown that the modeled spectra fit well with the observational ones of the October 28 burst at 11:05:30, 11:08:00, 11:16:00, and 11:20:15 UT (see solid lines). The physical parameters used in the spectral calculations are given in Table 3. We can

Table 2 Rising Rates r (sfu/GHz) of the Flux Density of the THz component at the Rise, Maximum Phase and Decay Phase for the three THz Bursts, measured from the observations at 210, 230/345 GHz (KOSMA) and at 212 and 405 GHz (SST).

date	time	Rise – phase	Max. – phase	Decay – phase	$S_{\sim 200\text{GHz}}$	$S_{345\text{or}405\text{GHz}}$	$r \text{ sfu/GHz}$
2003 10 28	11 : 03 : 15	yes			3.1×10^3		
	11 : 05 : 30		yes		1.1×10^4		
	11 : 16 : 00			yes	2.2×10^3	4.7×10^3	18.5
	11 : 20 : 15			yes	1.2×10^3	2.3×10^3	8.5
	11 : 25 : 00			yes	8.5×10^2	2.7×10^3	13.7
	11 : 29 : 00			yes	8.0×10^2	2.6×10^3	13.3
2003 11 02	17 : 16 : 15	yes			1.2×10^3	3.1×10^4	154
	17 : 17 : 06		yes		4.0×10^3	7.0×10^4	342
	17 : 17 : 30			yes	3.2×10^3	5.0×10^4	242
	17 : 18 : 00			yes	3.5×10^3	4.0×10^4	210
	17 : 18 : 30			yes	4.0×10^3	5.8×10^4	280
	17 : 19 : 00			yes	5.0×10^3	5.5×10^4	259
	17 : 19 : 30			yes	5.0×10^3	5.5×10^4	259
	17 : 20 : 00			yes	5.0×10^3	4.8×10^4	223
	17 : 21 : 00			yes	4.5×10^3	3.2×10^4	142
2003 11 04	19 : 42 : 40	yes			2×10^3	5×10^3	15.5
Peak 1	19 : 44 : 05		yes		1.15×10^4	2.0×10^4	44
Peak 2	19 : 45 : 20			yes	10^4	1.65×10^4	33.7
Peak 3	19 : 46 : 50			yes	10^4	1.5×10^4	25.9
Peak 4	19 : 48 : 25			yes	3.7×10^3	5.2×10^3	7.8

number density of electrons decreased substantially from 4.5×10^{10} to $4.5 \times 10^8 \text{ cm}^{-3}$ at the decay phase. The fit results for the MW spectra of the October 28 burst also be given in Table 3 during the burst for $E_0 = 10 \text{ keV}$ and $E_m = 5 \text{ MeV}$. At the decay phase the electron number density N in the MW source decreased from 6×10^7 to $1.5 \times 10^6 \text{ cm}^{-3}$, i.e., decreased by 40 times, but the value of N decreased by 100 times in the THz source. The total electron number N_{total} decreased by ~ 40 and ~ 400 times in the MW and THz source, respectively.

Another slowly rising THz burst on November 4 associated the largest soft X-ray burst ($X_{\geq 28}$) so far. However the associated rising THz spectral components are not so strong and the rising rates are only in the 7.8–44 rang (see Table 1), so it also belongs to a slowly rising THz burst. Their spectral fit results of the peak 1 and peak 4 had been given (see the original Figure 2 and Table 2 given by Zhou et al. 2011). The required the high-energy cutoff is also only 30 keV as the 2003 October 28 THz burst. The flux density reaches 11,500 sfu at 212 GHz at peak 1, which is close to the peak flux density of 11,000 sfu at 210 GHz of the October 28 burst, but the required electron number density for the November 4 burst is only 10^{10} cm^{-3} (see Table 3), which is only $\sim 1/5$ of the required value ($4.5 \times 10^{10} \text{ cm}^{-3}$) of the October 28 burst.

Table 3 Physical Parameters of Energetic Electrons for the Three Bursts

date	Time	δ	MW: R''	$N \text{ cm}^{-3}$	N_{total}	THz : R''	$N \text{ cm}^{-3}$	N_{total}
2003 10 28	11 : 05 : 30	2	25	6.0×10^7	2.0×10^{35}	0.5	4.5×10^{10}	5.9×10^{34}
	11 : 16 : 00	2.2	25	2.0×10^7	6.6×10^{34}	0.35	6×10^9	3.8×10^{33}
	11 : 20 : 15	1.9	25	1.5×10^6	4.9×10^{33}	0.25	4.5×10^8	1.5×10^{32}
2003 11 2	17 : 16 : 15	3	25	8.0×10^7	2.6×10^{35}	0.5	8×10^6	1.0×10^{31}
	17 : 17 : 06	3	25	1.8×10^8	5.9×10^{35}	0.5	4×10^8	5.2×10^{32}
	17 : 17 : 30	3	25	1.6×10^8	5.3×10^{35}	0.5	10^8	1.3×10^{32}
	17 : 18 : 00	3	25	1.6×10^8	5.3×10^{35}	0.5	4×10^7	5.2×10^{31}
	17 : 18 : 30	3	25	1.6×10^8	5.3×10^{35}	0.5	3×10^8	3.9×10^{32}
	17 : 19 : 00	3	25	1.5×10^8	5.0×10^{35}	0.5	2×10^8	2.6×10^{32}
	17 : 19 : 30	3	30	1.3×10^8	6.1×10^{35}	0.45	2×10^8	2.2×10^{32}
	17 : 20 : 00	3	30	1.3×10^8	6.1×10^{35}	0.45	1.3×10^8	1.4×10^{32}
	17 : 21 : 00	3	32	1.3×10^8	7.0×10^{35}	0.38	7×10^7	5.3×10^{31}
2003 11 4	P1	2.3	40	1.2×10^6	1.0×10^{34}	0.5	1.0×10^{10}	1.0×10^{34}
	P2	2.3	40	6.0×10^5	5.0×10^{33}	0.25	5.5×10^9	1.8×10^{33}

4.2 For the steeply rising THz burst

A giant rising THz burst detected on 2003 November 2 in the Super-AR NOAA 10486. Observations show that the flux density of the THz spectrum steeply rising and their rising rate of the flux density of the THz spectrum attained as high as 342 sfu/GHz at the maximum phase. Their mean rising rate also reached a value of 235 sfu/GHz (corresponding spectral index α of 4.8) during the burst (Li et al. 2015). The flux densities reached about 4,000 and 70,000 sfu at 212 and 405 GHz at the maximum phase respectively. The emissions at 405 GHz maintained continuous high level that they exceed largely the peak values of the microwave (MW) spectra during the main phase. Our studies suggest that such strong and steeply rising THz component can be produced by energetic electrons with a low-energy cutoff of 1 MeV via GS radiation in the magnetic dipole field case (Li et al. 2015). The electron number density N derived from our numerical fits, increased substantially from 8×10^6 to $4 \times 10^8 \text{ cm}^{-3}$ at the rise phase, i.e., N value increased 50 times at the rise phase (see Table 3). During the decay phase it decreased to $7 \times 10^7 \text{ cm}^{-3}$, i.e., decreased about five times from the maximum phase. The total electron number decreased an order of magnitude at the decay phase. Nevertheless in the MW emission source the N value decreased only by $\sim 30\%$ and the total electron number did not decrease but increased by $\sim 20\%$ at the decay phase.

The fit parameters at the maximum phase for the three radio events are given in Table 4. It is found from it that the required electron number density reaches $\sim 10^{10} \text{ cm}^{-3}$ for the two slowly rising THz burst spectra at the maximum phase, which is two orders of magnitude higher than that for the steeply increasing one. But for the steeply rising THz spectrum it requires a much higher low-energy cutoff of 1 MeV, while for the two slowly rising THz burst spectrum it only requires a 30 keV low-energy cutoff.

5 THE ENERGY FLUX OF ENERGETIC ELECTRONS

The energy flux and energy released by energetic electrons are important constraints on acceleration mech-

(Holman, 2003). Once the energy cutoffs and the number density of the energetic electrons are obtained from the numerical fit of observational spectrum, the distribution function of energetic electron $n(E)=GE^{-\delta}$ and the instantaneous energy flux E_F carried by energetic electrons can be determined as well. Here we will present a calculation formula of E_F for any time, including the relativistic correction factor γ (Lorentz factor) (c.f. Zhou et al. 1996; 2011) for the first time. It is

$$\begin{aligned} E_F &\simeq \frac{3.0G}{2.5-\delta}(E_m^{2.5-\delta} - E_0^{2.5-\delta})\gamma \quad (\delta \neq 2.5), \\ E_F &\simeq 3.0G \ln(E_m/E_0)\gamma \quad (erg \text{ cm}^{-2} \text{ s}^{-1})(\delta = 2.5). \end{aligned} \quad (1)$$

The G factor is

$$\begin{aligned} G &= \frac{N(\delta-1)}{(E_0^{1-\delta} - E_m^{1-\delta})} \quad (\delta \neq 1), \\ G &= N/\ln(E_m/E_0) \quad (\delta = 1). \end{aligned} \quad (2)$$

Lorentz factor γ is a function of electron energy. Here they are taken as 2 and 7.3 corresponding respectively to 500 keV and 3.2 MeV for the two slowly and a steeply rising THz bursts. Then we can estimate the instantaneous energy flux E_F at the maximum time putting these electron parameters (see Table 4) into the equations (1) and (2). The energy loss rate from the GS radiation, $E' \text{ erg s}^{-1}(=E_F \times A)$ can be estimated on the the source area A. Finally the energy $E \text{ erg}(=E' \times \Delta T)$ released by energetic electrons via the GS radiation can also be calculated on the lifetime ΔT (second) (full width at half maximum for the burst time profile). The estimated energy flux, energy loss rate, and energy released by energetic electrons are given in Table 5 in the THz and MW sources for the three bursts on the physical parameters given in Table 4.

Table 4 Parameters of the Burst Sources and Energetic Electrons at the Maximum Phase for the Three Rising THz Bursts.

date	$B_0(G)$	θ°	R''	δ	$E_0(keV)$	$E_m(MeV)$	$N(cm^{-3})$	N_{total}
2003 10 28 (THz)	5000	10	0.5	2.0	30	10	4.5×10^{10}	5.9×10^{34}
11 02	5000	60	0.5	3.0	1000	10	4×10^8	5.2×10^{32}
11 04	5000	80	0.5	2.3	30	10	10^{10}	1.3×10^{34}
2003 10 28 (MW)	2800	10	25	2.0	10	5	6×10^7	2.0×10^{35}
11 02	2800	60	25	3.0	10	5	1.8×10^8	5.9×10^{35}
11 04	2000	80	40	2.3	10	5	1.2×10^6	1.0×10^{34}

Table 5 shows that the energy flux E_F carried by the energetic electrons reached 1.5×10^{15} , 8×10^{14} , and $1.4 \times 10^{14} \text{ erg cm}^{-2} \text{ s}^{-1}$ at the maximum phase in the THz source for the three bursts, respectively. However in the MW source they only reached 2.4×10^{11} , 6.6×10^{10} , and $1.8 \times 10^9 \text{ erg cm}^{-2} \text{ s}^{-1}$ respectively, which are 3-5 orders of magnitude lower than that in the THz source. The energy loss rate E' reached, respectively, $6.1 \times 10^{30} - 5.7 \times 10^{29}$ and $4.8 \times 10^{28} - 2.5 \times 10^{30} \text{ erg s}^{-1}$ ranges in the THz source and in MW one at the maximum phase. It is found from Table 5 that although the modeled submillimeter source area is 3-4 orders of magnitude smaller than the modeled MW one, while the energy (E_{THz}) released by energetic electrons in the THz emission source exceeds that (E_{MW}) in microwave one. The ratio of E_{THz} to E_{MW} is 2.4, 5.0,

MW sources reached 3.8×10^{33} , 1.6×10^{33} , and 1.8×10^{32} erg for the October 28 burst, November 2 and 4 bursts, respectively (see Table 6). So in view of the radio energy the October 28 burst is the strongest for the three events.

Table 5 Energy Flux E_F , Energy Loss Rate E' , and Total Energy E Carried by Energetic Electrons vis the GS Radiation in the THz and MW Sources for the Three Submillimeter Bursts.

<i>date</i>	$N(cm^{-3})$	$E_F(erg\ cm^{-2}\ s^{-1})$	$E'(erg\ s^{-1})$	$\Delta T(s)$	$E(erg)$
2003 10 28(THz)	4.5×10^{10}	1.5×10^{15}	6.1×10^{30}	450	2.7×10^{33}
11 02	4.0×10^8	8.0×10^{14}	3.3×10^{30}	380	1.3×10^{33}
11 04	10^{10}	1.4×10^{14}	5.7×10^{29}	300	1.7×10^{32}
10 28 (MW)	6×10^7	2.4×10^{11}	2.5×10^{30}	450	1.1×10^{33}
11 02	1.8×10^8	6.6×10^{10}	6.9×10^{29}	380	2.6×10^{32}
11 04	1.2×10^6	1.8×10^9	4.8×10^{28}	300	1.4×10^{31}

6 DISCUSSION

6.1 Propagation effect

Although flux density at 210 GHz of the October 28 burst is smaller than the value at 212 GHz of the November 4 burst, the required electron number density reaches as high as $4.5 \times 10^{10}\ cm^{-3}$, which is 3.5 times higher than that of the November 4 burst maybe due to propagation effect. It was found that the emissivity of GS radiation increases with the propagation angle for the same harmonic number in the MW and millimeter range. And the increasing trend becomes more obviously (Zhou et al. 1999). In the THz range the propagation effect can be clarified by Figure 2. It shows the different GS emission spectra in the case of different propagation angles θ , where $\delta = 3$, $E_0 = 500\ keV$, $E_m = 10\ MeV$, and $N = 10^7\ cm^{-3}$. We can see from it that the flux densities at the higher frequencies in the THz range for $\theta = 80^\circ$ are, at least, one order of magnitude higher than those for $\theta = 20^\circ$. The propagation effect results in a higher electron number density requirement under the quasi-longitudinal propagation than that under the quasi-transverse one for a same observational flux density distribution.

6.2 Source size variation

We find that all the flux densities decreased rapidly in the THz range at decay phase for the three THz bursts. If we still take the same source size ($R = 0.''5$), then the required electron number N will decrease largely, which lead to the modeled flux densities of the GS emission at 345 or 405 GHz being always lower than the observational results, i.e., the modeled rising rate is smaller than that the observational one. So that the modeled GS spectrum can not fit the observational spectrum at higher frequencies. In this case we have to take a smaller source size of $0.''38$, $0.''35$, and even to $0.''25$ to fit these spectra in the decay phase for the three THz bursts, i.e., the THz source radius decreased by 20-50 % in the decay phase. The effect of the emission source size on the GS emission spectrum in the THz range is given (Li et al. 2015). On the contrary, we also found that the MW source size obtained from the spectrum fit increased from $25''$ to $32''$

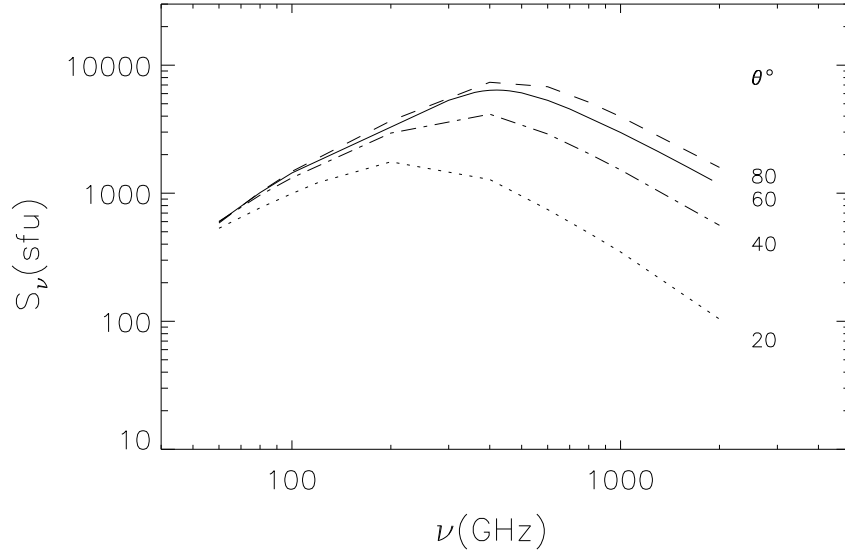


Fig. 2 The effect of the propagation angles θ° on the GS emission spectrum in submillimeter range, where $\delta = 3$, $E_0 = 500 \text{ keV}$, $E_m = 10 \text{ MeV}$, $N = 10^7 \text{ cm}^{-3}$, and $B_0 = 5000 \text{ G}$.

variation maybe is a rather interesting result. It would be a reflect of the various changes from the energetic electron acceleration, trapping, and the magnetic field topology in burst source.

6.3 Comparison of radio energy and thermal energy

The energy E_{THz} and E_{MW} released by energetic electrons of the October 28 burst in the THz and MW ranges can attain values of 2.7×10^{33} and $1.1 \times 10^{33} \text{ erg}$, respectively, which are the highest for the three bursts. The total radio energy E_R in the THz and MW ranges of the burst can reach $3.8 \times 10^{33} \text{ erg}$ due to a hard electron spectral index of 2 and a high electron number density of $4.5 \times 10^{10} \text{ cm}^{-3}$ (see Table 4). So in view of radio energy the October 28 burst is the strongest for the three events. The ratio of the radio energy to the thermal energy, E_R/E_T is 131 times for the October 28 burst, i.e., the radio energy is two orders of magnitude higher than that the thermal energy estimated from the soft X-ray GOES observations for the emission measure and temperature. For the November 2 burst E_{THz} reached only $1.3 \times 10^{33} \text{ erg}$ due to a narrower energy release range of electrons from 1 to 10 MeV and a mean electron number density. The value of E_R/E_T is 76 for this burst. For the November 4 burst the E_R/E_T value is only 4, because it is associated with the largest soft X-ray flare so far and the estimated thermal energy attained $5.2 \times 10^{31} \text{ erg}$.

6.4 Comparison of the modeled spectra of the three radio bursts

Figure 3 shows a comparison of the three modeled GS spectra fitting the observations of the October 28, November 2 and 4 bursts over interval of the maximum phase or at the maximum phase. It shows that the MW emission of the October 28 burst is the strongest for the three bursts, because it is produced by the energetic electrons with a harder spectral index ($\delta = 2$). While the THz emission of the October 28 burst appears to be lower, although the observational flux density at 210 GHz is close to that of the another two

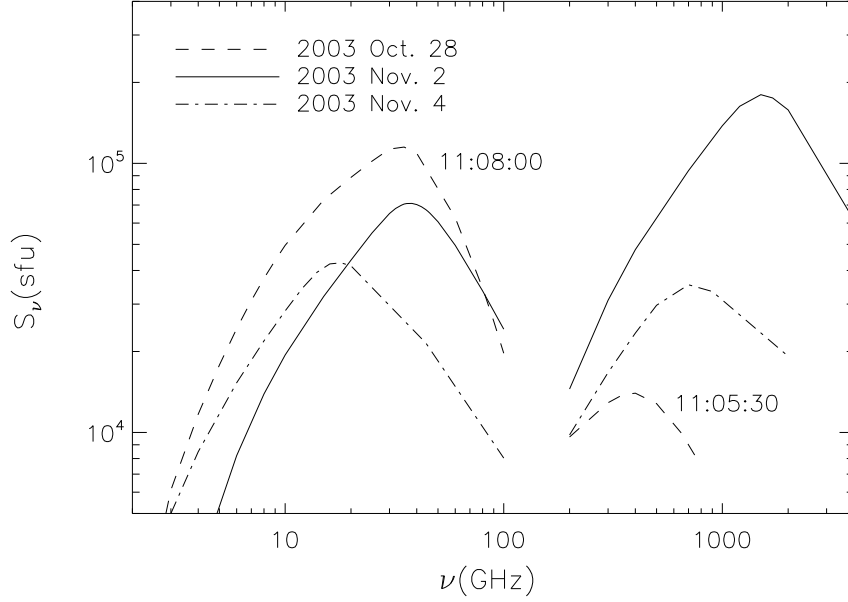


Fig. 3 The modeled spectra for the observations at 11:08:00 and 11:05:30 UT over interval of the maximum phase of the 2003 October 28 burst, at 17:17:06 UT of the maximum phase of the November 2 burst, and at the peak 1 of the maximum phase of the November 4 burst (Zhou et al. 2011).

obtained during the main phase. So we only give an increasing THz spectrum component with a smaller rising rate, which leads to an underestimated model spectrum. For the November 2 burst the modeled THz emission is the strongest among the three bursts and this peak frequency reaches 1440 GHz, due to intense ultra-relativistic electron GS radiation in a higher energy emission range of 1-10 MeV under the quasi-transverse propagation condition. It is shown from the comparison of the modeled spectra of the three THz bursts that the emission strengths are very different for the three bursts and for the different emission frequency ranges, which depends strongly on the electron acceleration and various physical conditions of burst region.

Table 6 Total Radio Energy $E_R(erg)$ Carried by Energetic Electrons and the Thermal Energy $E_T(erg)$ Estimated from the Soft X-Ray GOES Observations.

date	$E_{THz}(erg)$	$E_{MW}(erg)$	E_{THz}/E_{MW}	$E_R(erg)$	$E_T(erg)$	E_R/E_T
2003 10 28	2.7×10^{33}	1.1×10^{33}	2.4	3.8×10^{33}	2.9×10^{31}	131
11 02	1.3×10^{33}	2.6×10^{32}	5.0	1.6×10^{33}	2.1×10^{31}	76
11 04	1.7×10^{32}	1.4×10^{31}	12	1.8×10^{32}	5.2×10^{31}	4

7 CONCLUSIONS

In the paper we investigate the three novel rising submillimeter bursts occurring in the Active Region NOAA 10486. It is found from the numerical fit that the two slowly rising and a steeply rising submillimeter spectral

ranges in a compact source (about $0.''5$ radius) with strong local magnetic fields varying from 4590 to 780 G via the GS emission. The photosphere magnetic field of 5000 G would be possible on observation in a compact source (Li et al. 2015). The associated microwave spectral components can be produced by energetic electrons with 10 keV–5 MeV and with a mean local magnetic field strength in an extend source of $25''$ – $40''$ radius.

It is found from the spectral temporal evolution that the number density variation amplitude is much larger in the THz source than that in the MW source during the bursts. The dramatic variation of electron number density in the THz source could result from the effective electron acceleration in the rise phase and strong electron energy loss during the flare. While in the MW source the variation amplitude of electron number density is one order of magnitude lower than that in the THz source. Because in the MW source there are much more electrons decayed from the higher energy to lower energy and less electron energy loss. The instantaneous energy flux of electrons in the THz source is about 4–5 orders of magnitude higher than that in microwave one for the three bursts. Although the modeled THz source area is 3–4 orders of magnitude smaller than the modeled MW one, the energies released by energetic electrons in the THz source are 2–12 times of those in microwave source due to the strong GS radiation loss at the submillimeter wavelengths. The total energies released by energetic electrons via the GS radiation in the MW and THz sources are estimated, respectively, to be 3.8×10^{33} , 1.6×10^{33} and 1.8×10^{32} erg for the October 28, November 2 and 4 bursts, which are 131, 76, and 4 times as large as the thermal energies of 2.9×10^{31} , 2.1×10^{31} and 5.2×10^{31} erg estimated from the soft X-ray GOES observations.

Our investigations show that the detailed GS emission models fit well with the rising submillimeter spectral components for the three novel submillimeter bursts. So this submillimeter spectral component could provide important diagnostics about the high relativistic electrons with higher energy rang of a few tens keV– ~ 10 MeV and their environment in burst regions. Further more, it is found from the modeled calculations that the THz source radius decreased by 20–50% during the decay phase for the three events, but the MW one increased by 28% for the 2003 November 2 event. The interesting result about source size variations maybe is significant for the studies about energetic electron acceleration, trapping, and magnetic field construction variation of source region. However we must note that the required source radius is usually much smaller, based on the GS emission calculations. Further progress in understanding the physics of THz emission from flares requires more observations with a complete spectral coverage at the THz range, such as the Atacama Large Millimeter/Submillimeter Array (ALMA).

Acknowledgements The authors thank Dr. V. F. Melnikov for fruitful discussions. This study is supported by the NFSC project with Nos. 11333009 and 11573072, the “973” program with No. 2014CB744200.

References

- Bastian, T. S., Benz, A. O., & Gary, D. E. 1998, ARA&A, 36, 131
- Dulk, G. A. 1985, ARA&A, 23, 169
- Holman, G. D. 2003, ApJ, 586, 606
- Kane, S. R., McTiernan, J. M., & Hurley, K. 2005, A&A, 433, 1133
- Kaufmann, P., et al. 2004, ApJ, 603, L121
- Krucker, S., Giménez de Castro, C. G., Hudson, H. S., et al. 2013, A&A Rev., 21, 58

- Lüthi, T., Lüdi, A., & Magun, A. 2004a, A&A, 420, 361
- Lüthi, T., Magun, A. & Miller, M. 2004b, A&A, 415, 1123
- Miller, J. A., et al. 1997, J. Geophys. Res., 102, 14631
- Pick, M., Klein, K.-L., & Trottet, G. 1990, ApJS, 73, 165
- Ramaty, R., Schwartz, R. A., Enome, S., & Nakajima, H. 1994, ApJ, 436, 941
- Silva, A. V. R., Share, G. H., Murphy, R. J., Costa, J. E. R., de Castro, C. G. G., Raulin, J.-P., & Kaufmann, P. 2007, Sol. Phys., 245, 311
- Trottet, G., Krucker, S., Lüthi, T., & Magun, A. 2008, ApJ, 678, 509
- Zhou, A.-H., Zhang, J., & Zhang, H. 1996, Chinese Science Bulletin, 41, 671
- Zhou, A.-H., Huang, G. L., & Wang, X.-D. 1999, Sol. Phys., 189, 345
- Zhou, A.-H., Li, J.-P., & Wang, X.-D. 2008, Sol. Phys., 247, 63
- Zhou, A. H., Huang, G. L., & Li, J. P. 2010, ApJ, 708, 445
- Zhou, A. H., Li, J. P., & Wang, X. D. 2011, ApJ, 727, 42
-